Arch. Mech., 38, 1-2, pp. 39-58, 1986

Drum shell under concentrated forces tangential to its edge and middle surface with various boundary conditions

T. KACPERSKI and R. K. MOŁDACH (WARSZAWA)

THE PAPER deals with the analysis of a semi-infinite drum shell loaded by concentrated forces tangential to the free edge and the middle surface of a shell. Moreover, the forces act edgewise in the same direction. The formulae, based on the Donnell–Vlasov equations, are derived for three types of boundary conditions. Numerical computation for the case of loading by the couple of forces acting at two opposite points of the boundary is made for the simply supported edge. The components of the displacements as well as internal moments and forces are given.

Przeprowadzono analizę półnieskończonej powłoki cylindrycznej obciążonej siłami skupionymi stycznymi do jej brzegu swobodnego oraz do powierzchni środkowej. Siły działają ponadto stycznie do brzegu w tym samym kierunku. Wzory oparte na równaniach Donnella–Własowa wyprowadzono dla trzech typów warunków brzegowych. Obliczenia numeryczne przeprowadzono dla przypadku brzegu swobodnie podpartego. Podano składowe przemieszczeń, momentów i sił wewnętrznych wywołanych w powłoce.

Проанализирована полубесконечная цилиндрическая оболочка, нагруженная сосредоточенными силами, касательными к её свободному краю и к центральной поверхности. Кроме того, силы действуют касательно к краю в том же направлении. На основе уравнений Доннелля–Власова выведены формулы для граничных условий трех типов. Числовые расчеты произведены для случая свободно опертого края. Приведены составляющие перемещений, моментов и внутренних сил, возникающих в оболочке

1. Introduction

THE SOLUTION of the propulsion transmission with the aid of a cylindrical sleeve loaded by concentrated forces, found in many civil engineering constructions, is directly related to basic questions which must be answered. The most important of them are: what deformations take place, what is important from the point of view of proper bearing localization, and what is the stress concentration. These questions can be answered with sufficient accuracy for most of technical applications, using the DONNELL–VLASOV [1, 2] shell theory or the theory improved by Łukasiewicz [3]. Another problem is what boundary conditions should be assumed to represent the actual supports. This was the essential reason for analysing three types of boundary conditions in the present paper. Similar problems are analysed in [4]; however, full results and formulae for this technically important case have not been given. The solutions for a semi-infinite circular cylindrical shell loaded by concentrated forces normal to its edge and tangential to the middle surface for two boundary conditions, the free edge and supported by means of an articulated joint, are given in the papers [5, 6]. The Donnell–Vlasov equations were used to solve the problem. For the case described in [5], experimental research, the results of which confirm numerical computations was carried out. The derivation of formulae for internal forces and moments as well as displacements of a semi-infinite drum shell loaded by concentrated forces is the main purpose of the paper. The concentrated forces are tangential to the free edge and middle surface of the shell and act in the same direction. The Donnell–Vlasov equations constitute the basis for the analysis being presented.

2. Theoretical solution

Consider a thin-walled circular cylindrical shell under the action of concentrated forces tangential to its edge and the middle surface. The three types of boundary conditions will be analysed: free edge (Fig. 1a), simply-supported edge (Fig. 1b), and the sliding support (Fig. 1c). The set of two Donnell–Vlasov differential equations of the fourth order

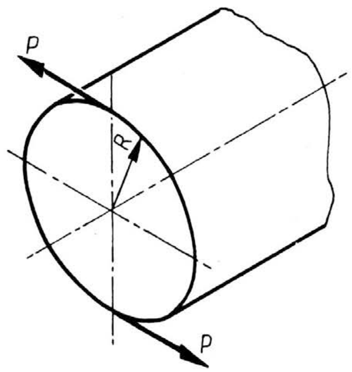

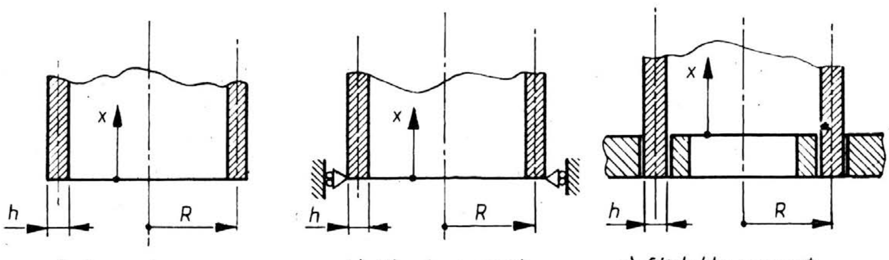

FIG. 1.

$$D\Delta\Delta w - \Delta_k \Phi = 0,$$
(2.1)
$$\frac{1}{Eh}\Delta\Delta\Phi + \Delta_k w = 0,$$

describes such a shell with sufficient accuracy for engineering purposes. Here D — bending rigidity, $D = Eh^3/(12(1-\nu^2))$, E — Young's modulus, ν — Poisson ratio, Φ — stress function, w — radial shell displacement, Δ — Laplace operator which, for a circular cylindrical shell, reads $\Delta = \partial^2/\partial x^2 + \partial^2/R^2\partial\varphi^2$ Δ_k — operator, $\Delta_k = \partial^2/R\partial x^2$.

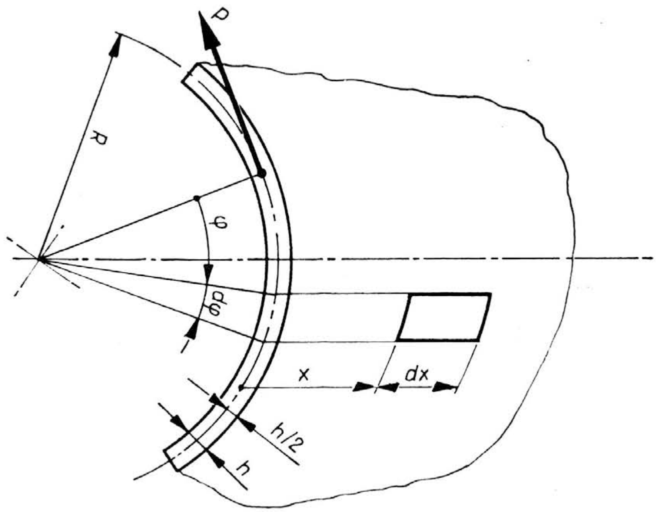

FIG. 2.

For the remaining notations see Fig. 2.

The shell deflection w and the stress function Φ for the loading considered may be represented in form of the series

$$(2.2)\qquad w = \sum_{n=1}^{\infty} e^{k\frac{x}{R}} \sin n\varphi, \qquad \Phi = \sum_{n=1}^{\infty} \lambda e^{k\frac{x}{R}} \sin n\varphi.$$

Substituting the relations (2.2) into the set (2.1), one obtains the set of two algebraic equations with the unknown quantities λ and k

$$(2.3)\qquad D(k^2-n^2)^2 - \lambda Rk^2 = 0, \qquad \lambda(k^2-n^2)^2 + EhRk^2 = 0.$$

Furthermore, after λ has been eliminated, one gets the following form of the characteristic equation:

$$(2.4)\qquad (k^2-n^2)^4 + 4\varkappa^4 k^4 = 0,$$

whose solution reads

$$(2.5)\qquad k_{1\cdots 8} = \frac{\varkappa}{2}\left[[\pm]1(\pm)\sqrt{\xi+\delta} \pm i\left([\pm]1(\pm)\sqrt{\xi-\delta}\right)\right],$$

where

$$\varkappa^2 = \frac{R}{h}\sqrt{3(1-\nu^2)},$$

$$\delta = 2n^2/\varkappa^2,$$

$$\xi = \sqrt{1+\delta^2},\qquad i = \sqrt{-1}. \tag{2.6}$$

The signs appearing in similar brackets in Eq. (2.5) should be the same.

After the quantity k has been eliminated from Eqs. (2.3), the formula defining λ takes the form

$$\lambda = \pm 2i\varkappa^2 D/R. \tag{2.7}$$

In Eq. (2.7) the plus sign corresponds to the odd roots and the minus sign to the even ones (cf. Eqs. (2.9)). The deflection w and the stress function Φ may be expressed in the form

$$\begin{aligned} w &= \sum_{n=1}^{\infty}\sum_{j=1}^{8} A_j e^{k_j \frac{x}{R}} \sin n\varphi, \\ \Phi &= \sum_{n=1}^{\infty}\sum_{j=1}^{8} \lambda A_j e^{k_j \frac{x}{R}} \sin n\varphi. \end{aligned} \tag{2.8}$$

It is convenient to represent the roots k_j in the form

$$\begin{aligned} k_1 &= \frac{\varkappa}{2}(b+ia), & k_5 &= \frac{\varkappa}{2}(-b+ia), \\ k_2 &= \frac{\varkappa}{2}(b-ia), & k_6 &= \frac{\varkappa}{2}(-b-ia), \\ k_3 &= \frac{\varkappa}{2}(d+ic), & k_7 &= \frac{\varkappa}{2}(-d+ic), \\ k_4 &= \frac{\varkappa}{2}(d-ic), & k_8 &= \frac{\varkappa}{2}(-d-ic), \end{aligned} \tag{2.9}$$

where

$$\begin{aligned} a &= 1-\sqrt{\xi-\delta}, \\ b &= 1-\sqrt{\xi+\delta}, \\ c &= -\left(1+\sqrt{\xi-\delta}\right), \\ d &= -\left(1+\sqrt{\xi+\delta}\right). \end{aligned} \tag{2.10}$$

Since the semi-infinite circular shell is considered and due to the character of the exponential function, the constants $A_{5...8}$ relating to the roots $k_{5...8}$, whose real parts are positive, are assumed to be equal to zero. Displacements and stresses cannot increase exponential by with increasing x.

The components of internal forces and moments as well as displacements are marked in Fig. 3. Knowledge of the deflection w enables the remaining displacement components u and v to be computed from the following relations:

$$\begin{aligned} R^4\Delta\Delta u &= -R^3\nu\frac{\partial^3 w}{\partial x^3} + R\frac{\partial^3 w}{\partial x\,\partial\varphi^2}, \\ R^4\Delta\Delta v &= -R^2(2+\nu)\frac{\partial^3 w}{\partial x^2\,\partial\varphi} - \frac{\partial^3 w}{\partial\varphi^3}. \end{aligned} \tag{2.11}$$

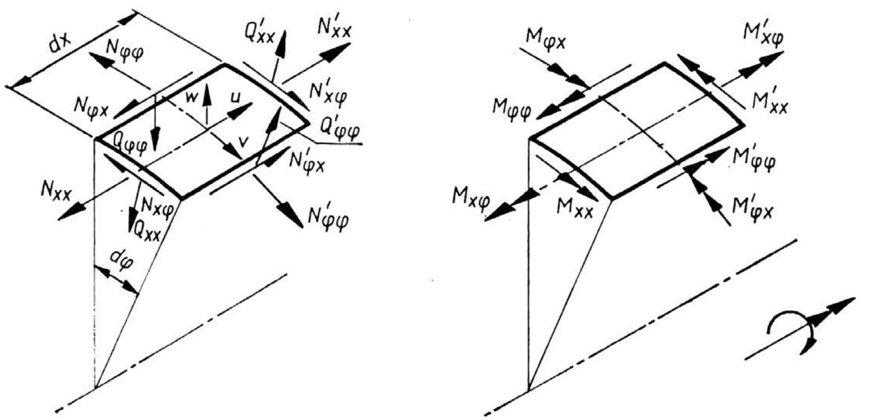

FIG. 3.

Furthermore, the internal moments and shearing forces read

(2.12)
$$M_{xx} = -D\left(\frac{\partial^2 w}{\partial x^2} + \frac{\nu}{R^2}\frac{\partial^2 w}{\partial \varphi^2}\right),$$
$$M_{\varphi\varphi} = -D\left(\frac{\partial^2 w}{R^2 \partial \varphi^2} + \nu\frac{\partial^2 w}{\partial x^2}\right),$$
$$M_{x\varphi} = -(1-\nu)\frac{D}{R}\frac{\partial^2 w}{\partial x \partial \varphi},$$
$$Q_{xx} = -D\left(\frac{\partial^3 w}{\partial x^3} + \frac{1}{R^2}\frac{\partial^3 w}{\partial x \partial \varphi^2}\right),$$
$$Q_{\varphi\varphi} = -D\left(\frac{\partial^3 w}{R\partial x^2 \partial \varphi} + \frac{1}{R^3}\frac{\partial^3 w}{\partial \varphi^3}\right).$$

The membrane forces are defined by means of the stress function Φ

(2.13)
$$N_{xx} = -\frac{1}{R^2}\frac{\partial^2 \Phi}{\partial \varphi^2},$$
$$N_{\varphi\varphi} = -\frac{\partial^2 \Phi}{\partial x^2},$$
$$N_{x\varphi} = \frac{1}{R}\frac{\partial^2 \Phi}{\partial x \partial \varphi}.$$

Assuming

(2.14)
$$u = \sum_{n=1}^{\infty}\sum_{j=1}^{4} B_j e^{k_j \frac{x}{R}} \cos n\varphi,$$
$$v = \sum_{n=1}^{\infty}\sum_{j=1}^{4} C_j e^{k_j \frac{x}{R}} \sin n\varphi.$$

and taking advantage of Eqs. (2.11), one gets the following relations between the constants B_j, C_j and A_j:

$$
B_j = -\frac{\nu k_j^2+n^2}{(k_j^2-n^2)^2}\, k_j A_j, \tag{2.15}
$$

$$
C_j = \frac{n^2-(2+\nu)k_j^2}{(k_j-n^2)^2}\, nA_j.
$$

Substituting the relations (2.8) into Eqs. (2.12) and (2.13), one obtains the following formulae defining the internal moments and forces:

$$
M_{xx} = -\frac{D}{R^2}\sum_{n=1}^{\infty}\sum_{j=1}^{4} A_j e^{k_j\frac{x}{R}}(k_j^2-\nu n^2)\sin n\varphi,
$$

$$
M_{\varphi\varphi} = -\frac{D}{R^2}\sum_{n=1}^{\infty}\sum_{j=1}^{4} A_j e^{k_j\frac{x}{R}}(\nu k_j^2-n^2)\sin n\varphi,
$$

$$
M_{x\varphi} = -\frac{D}{R^2}(1-\nu)\sum_{n=1}^{\infty} n\sum_{j=1}^{4} A_j e^{k_j\frac{x}{R}} k_j\cos n\varphi,
$$

$$
Q_{xx} = -\frac{D}{R^3}\sum_{n=1}^{\infty}\sum_{j=1}^{4} A_j e^{k_j\frac{x}{R}} k_j(k_j^2-n^2)\sin n\varphi,
$$

$$
Q_{\varphi\varphi} = -\frac{D}{R^3}\sum_{n=1}^{\infty} n\sum_{j=1}^{4} A_j e^{k_j\frac{x}{R}}(k_j^2-n^2)\cos n\varphi, \tag{2.16}
$$

$$
N_{xx} = -\frac{1}{R^2}\sum_{n=1}^{\infty} n^2\sum_{j=1}^{4} \lambda A_j e^{k_j\frac{x}{R}}\sin n\varphi,
$$

$$
N_{\varphi\varphi} = -\frac{1}{R^2}\sum_{n=1}^{\infty}\sum_{j=1}^{4} \lambda A_j e^{k_j\frac{x}{R}} k_j^2\sin n\varphi,
$$

$$
N_{x\varphi} = -\frac{1}{R^2}\sum_{n=1}^{\infty} n\sum_{j=1}^{4} \lambda A_j e^{k_j\frac{x}{R}} k_j\cos n\varphi.
$$

At the edge of a shell one has to define four boundary conditions which, for every number n, will enable the computation of the constants $A_{1\ldots4}$. Hence, for each of three (Figs. 1a, b, c) boundary conditions, four relations should be chosen from the following equations:

$$
\left[N_{x\varphi}+\frac{M_{x\varphi}}{R}\right]_{x=0} = P\delta(\varphi),
$$

$$
\left[Q_{xx}+\frac{\partial M_{x\varphi}}{R\partial\varphi}\right]_{x=0} = 0,
$$

$$
\begin{aligned}
[M_{xx}]_{x=0} &= 0,\\
[N_{xx}]_{x=0} &= 0,\\
[w]_{x=0} &= 0,\\
\left[\frac{\partial w}{\partial x}\right]_{x=0} &= 0,
\end{aligned}
\tag{2.17}
$$

where $\delta(\varphi)$ is the Dirac delta function.

Substitution of the formulae (2.16) into Eqs. (2.17) yields the conditions for $n \geqslant 1$

$$
\begin{aligned}
\sum_{j=1}^{4} -A_j k_j\big((-1)^j 2i\varkappa^2+1-\nu\big) &= \frac{mPR^2}{\pi D n},\\
\sum_{j=1}^{4} A_j k_j\big(-k_j^2+n^2(2-\nu)\big) &= 0,\\
\sum_{j=1}^{4} A_j(k_j^2-\nu n^2) &= 0,\\
\sum_{j=1}^{4} (-1)^j A_j &= 0,\\
\sum_{j=1}^{4} A_j &= 0,\\
\sum_{j=1}^{4} k_j A_j &= 0,
\end{aligned}
\tag{2.18}
$$

where m is a number of the uniformly spaced points at the circumference, each one loaded by the force P. For each boundary condition Eqs. (2.18) should be chosen according to Table 1.

Table 1

Equation	$(2.18)_1$	$(2.18)_2$	$(2.18)_3$	$(2.18)_4$	$(2.18)_5$	$(2.18)_6$
free edge	YES	YES	YES	YES	NO	NO
simply-supported	YES	NO	YES	YES	YES	NO
sliding support	YES	NO	NO	YES	YES	YES

(diagonally crossed box = YES; empty box = NO)

In Eqs. (2.8), (2.14), (2.16) and (2.18), n takes the values of subsequent multiples of m (for instance, if $m = 2$, then $n = 2, 4, 6, \ldots$).

After the set of Eqs. (2.18) has been solved, the internal moments and forces are computed with the aid of the formulae (2.16), the deflection w from Eq. (2.8) and the remaining displacements u, v from Eqs. (2.14).

However, this is not the complete solution because it does not include the case $n = 0$. It has been assumed that in this case, this means for edge loaded by the uniform shearing unit force $p_0 = mP/2\pi R$, the only nonvanishing quantities are the displacement u, which is expressed by the unit torsional deflection θ, and the internal force $N_{x\varphi}$. In the present case these take the form

$$\theta = \frac{mP(1+\nu)}{\pi EhR^2}, \qquad N_{x\varphi} = \frac{mP}{2\pi R}. \tag{2.19}$$

Applying the described technique, one obtains the solution in terms of complex quantities as a sum of series whose real and imaginary parts are equal to each other.

3. Numerical solution

The computations of displacements, internal forces and moments were made in the case of a simply supported shell loaded by two forces (see Fig. 1b). It was assumed $R/h = 10$ and $\nu = 0.3$. The results are presented in nondimensional units and coordinates

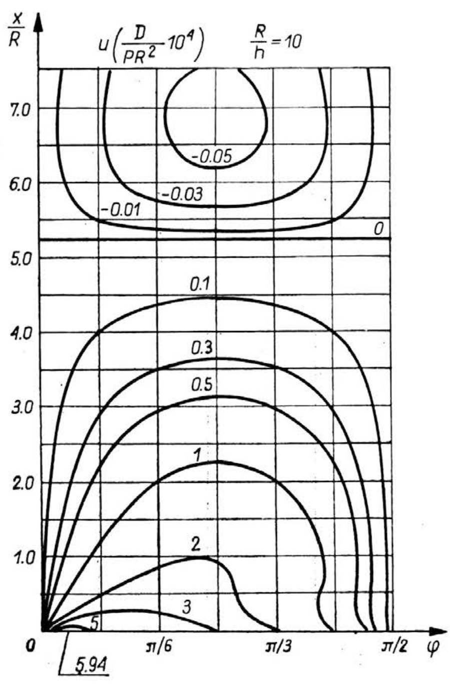

FIG. 4.

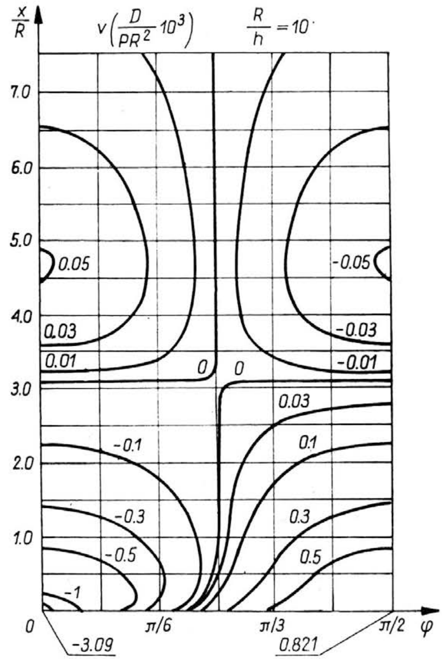
x/R
$v\left(\frac{D}{pR^2}10^3\right)$
$\frac{R}{h}=10$
7.0
6.0
5.0
4.0
3.0
2.0
1.0
0
0.05
-0.05
0.03
-0.03
0.01
-0.01
0
0
0.03
-0.1
0.1
-0.3
0.3
-0.5
0.5
-1
π/6
π/3
π/2
φ
-3.09
0.821

FIG. 5.

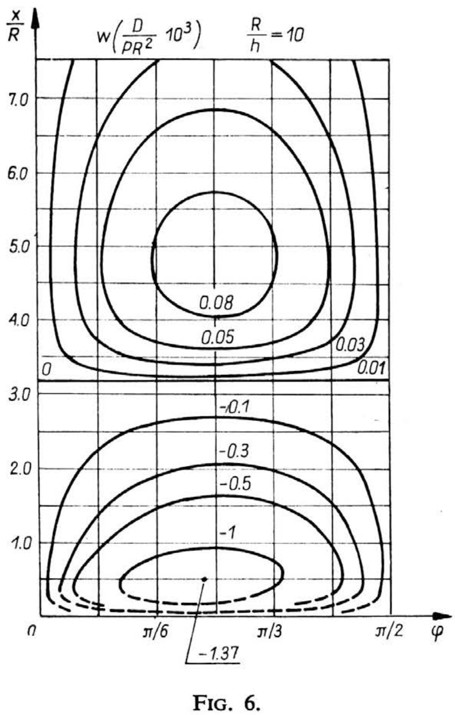
x/R
$w\left(\frac{D}{pR^2}10^3\right)$
$\frac{R}{h}=10$
7.0
6.0
5.0
4.0
3.0
2.0
1.0
0.08
0.05
0.03
0
0.01
-0.1
-0.3
-0.5
-1
0
π/6
π/3
π/2
φ
-1.37

FIG. 6.

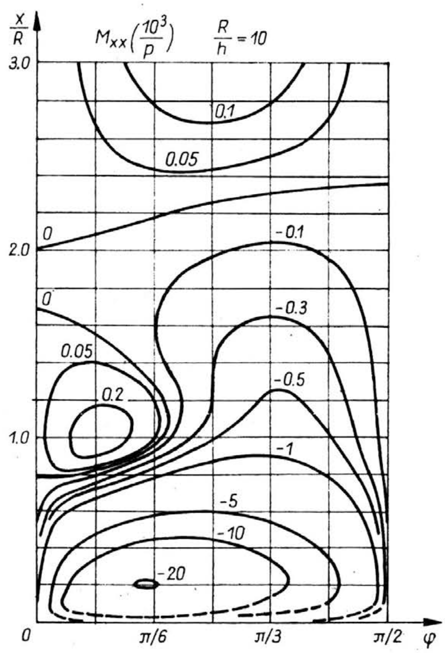

x/R
Mxx (10^3/p)
R/h = 10
3.0
0.1
0.05
0
2.0
-0.1
0
-0.3
0.05
-0.5
0.2
1.0
-1
-5
-10
-20
0
π/6
π/3
π/2
φ

FIG. 7.

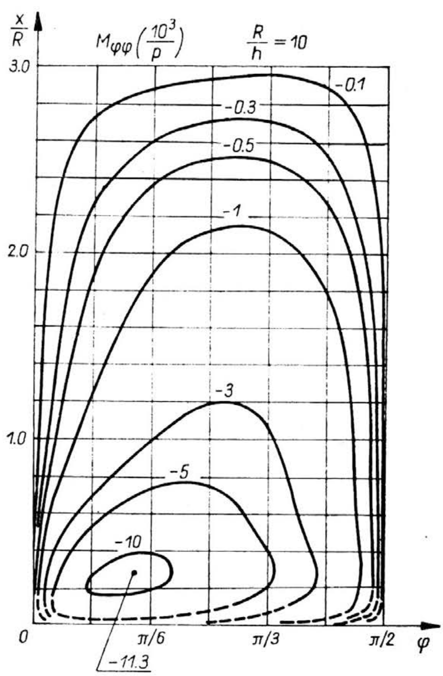

x/R
Mφφ (10^3/p)
R/h = 10
3.0
-0.1
-0.3
-0.5
-1
2.0
-3
1.0
-5
-10
0
π/6
π/3
π/2
φ
-11.3

FIG. 8.

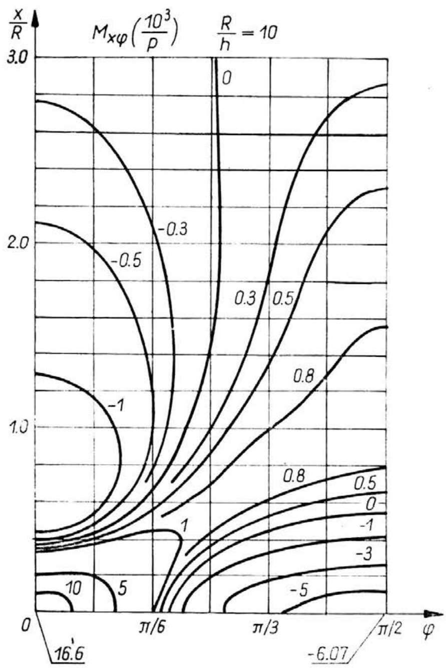

x/R
$M_{x\varphi}\left(\frac{10^3}{p}\right)$
R/h = 10
3.0
2.0
1.0
0
0
-0.3
-0.5
0.3
0.5
0.8
-1
0.8
0.5
0
-1
-3
-5
1
10
5
π/6
π/3
π/2
φ
16.6
-6.07

FIG. 9.

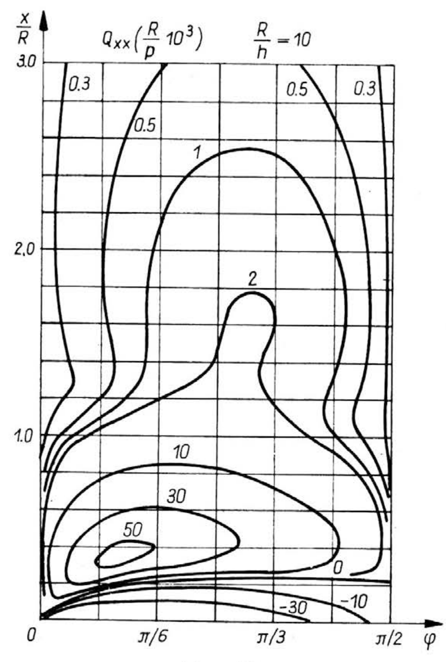

x/R
$Q_{xx}\left(\frac{R}{p}10^3\right)$
R/h = 10
3.0
2.0
1.0
0
0.3
0.5
1
2
0.5
0.3
10
30
50
0
-10
-30
π/6
π/3
π/2
φ

FIG. 10.

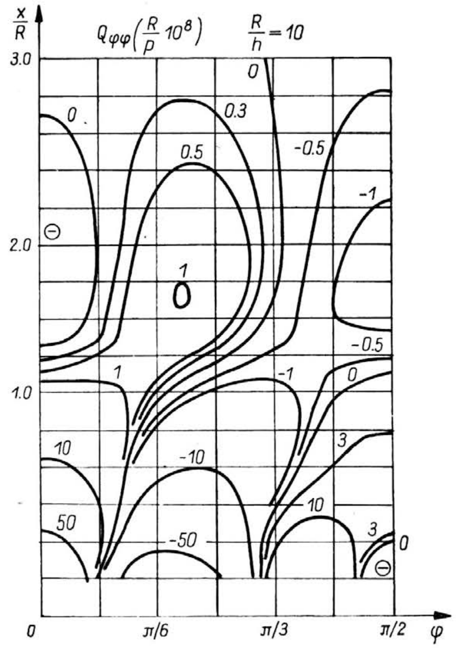

x/R
$Q_{\varphi\varphi}\left(\frac{R}{p}10^8\right)$
$\frac{R}{h}=10$
3.0
2.0
1.0
0
π/6
π/3
π/2
φ
0
0.3
0.5
-0.5
-1
1
-0.5
1
-1
0
3
10
-10
50
-50
10
3
0

FIG. 11.

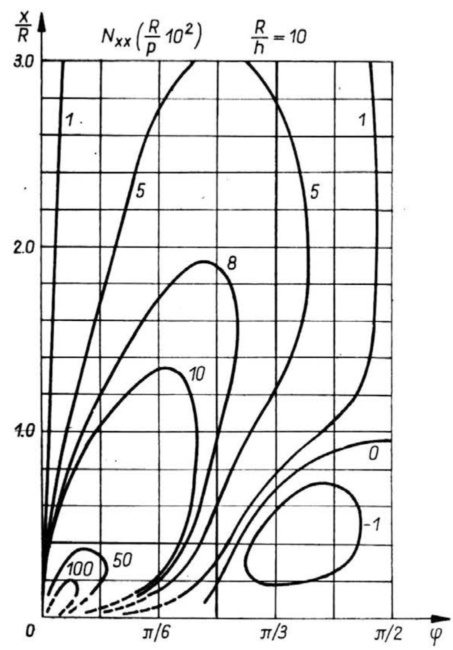

x/R
$N_{xx}\left(\frac{R}{p}10^2\right)$
$\frac{R}{h}=10$
3.0
2.0
1.0
0
π/6
π/3
π/2
φ
1
5
5
1
8
10
0
-1
100
50

FIG. 12.

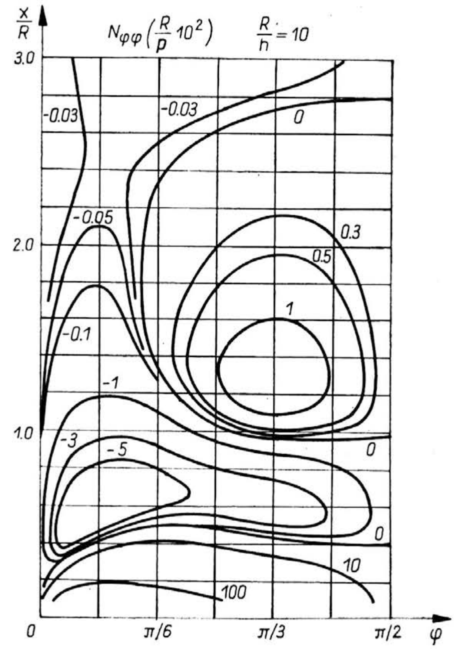

FIG. 13.

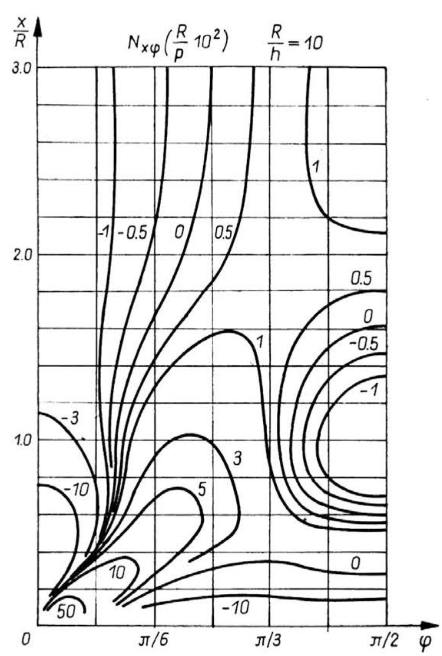

FIG. 14.

4*

what makes it possible for them to be used for an arbitrary shell of such a proportion and material. For other shells it is necessary to make separate computations. The detailed analysis of accuracy and convergence is presented in Sect. 4.

Figures 4–14 present the displacements u, v, w and the internal moments and forces M_{xx}, $M_{\varphi\varphi}$, $M_{x\varphi}$, Q_{xx}, $Q_{\varphi\varphi}$, N_{xx}, $N_{\varphi\varphi}$, $N_{x\varphi}$. They were made for higher harmonics and for $\varphi \in (0, \pi/2)$. In the remaining quadrants the functions are symmetric or anti-symmetric, according to the character of the functions $\cos 2\varphi$ or $\sin 2\varphi$ appearing in Eqs. (2.8), (2.14), and (2.16). In order to complete the results, one should add to $N_{x\varphi}$ and v the harmonic $n = 0$ using the formulae (2.19). In order to obtain the moment stresses σ_M and membrane stresses σ_N, one should use the following formulae:

$$\sigma_M = \pm \frac{6M}{h^2}, \qquad \sigma_N = \frac{N}{h}, \tag{3.1}$$

where M_{xx} or $M_{\varphi\varphi}$ are substituted for M, and N_{xx}, $N_{\varphi\varphi}$ or $N_{x\varphi}+M_{x\varphi}/R$ for N.

4. Analysis of convergence

It is a well-known fact that in the case of thin-walled shells under concentrated load, the solutions obtained by summation of the infinite series are slowly convergent. With the aim of evaluating a minimum number of terms of the series, the convergence analysis was made. The values of the displacements, internal moments and forces were computed for different numbers of terms of the series. Besides, for each of these components only one chosen value φ was taken into account. The angle φ was fitted in such a way that the corresponding generator included a point in which the function value was minimum or

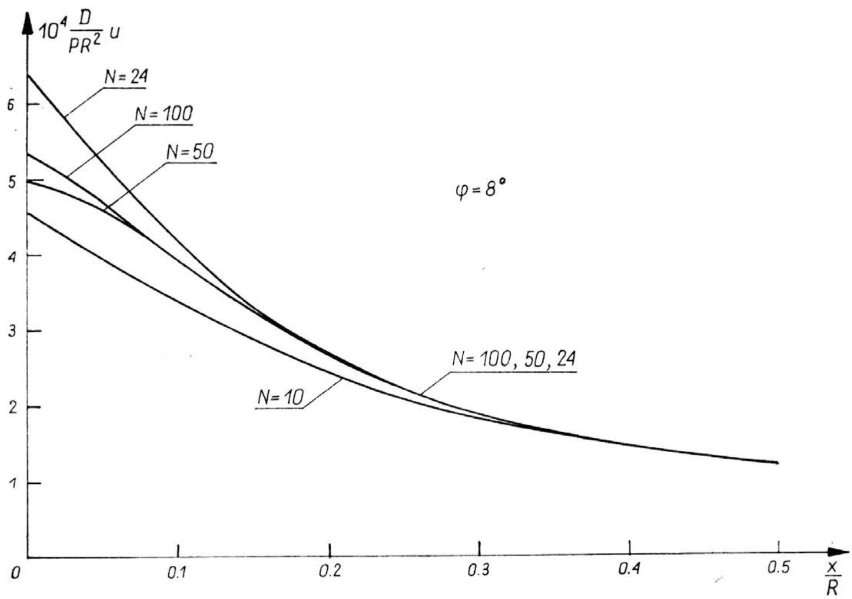

FIG. 15.

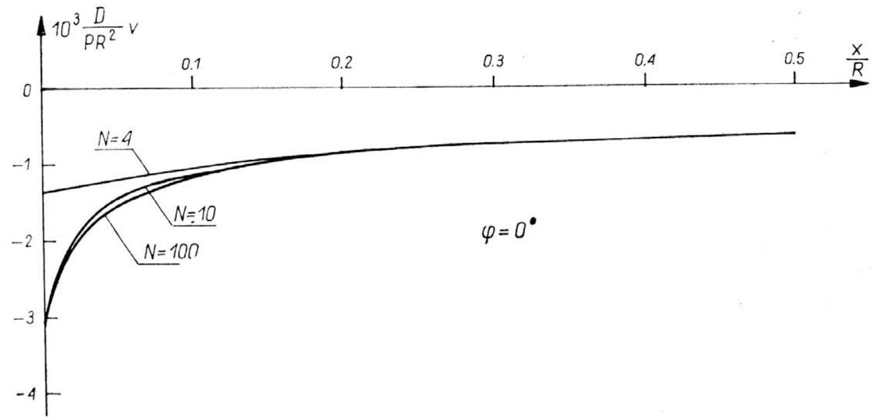

FIG. 16.

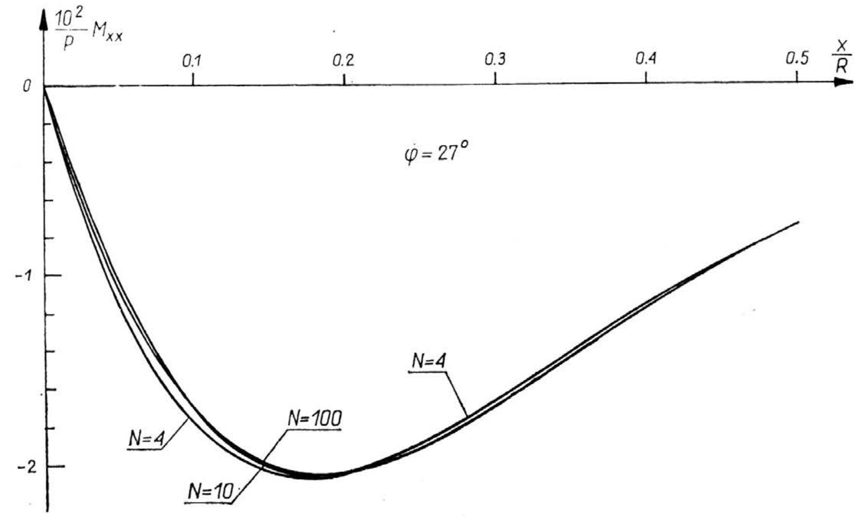

FIG. 17.

maximum. Figures 15–25 show the results of this analysis. As it is easy to observe, for x/R greater than 0.5 the limitation of summation up to $N = 10$ gives satisfactory results. Since the number of forces is two, this means that in this case only five elements of the series are considered. The same situation takes places for x/R less than 0.5 in the case of the displacements v and w, internal moments M_{xx} and $M_{\varphi\varphi}$ and the force Q_{xx}. The evidence of good convergence gives also the displacement u and the moment $M_{x\varphi}$. The remaining quantities $Q_{\varphi\varphi}$, N_{xx}, $N_{\varphi\varphi}$, $N_{x\varphi}$, especially for x/R less than 0.1, are slowly convergent. This is easy to explain only in the case of $N_{x\varphi}$, which for the chosen angle $\varphi = 0°$ and for $x/R = 0.0$ takes an infinite value. Because of this, in Figs. 11, 13, and 14 no lines are plotted near $x/R = 0.0$. The dashed line used in Figs. 6, 7, 8 and 12 appears since the computed values for $x/R = 0.0$ were not exact zero but 10^4–10^6 times less than the greater ones.

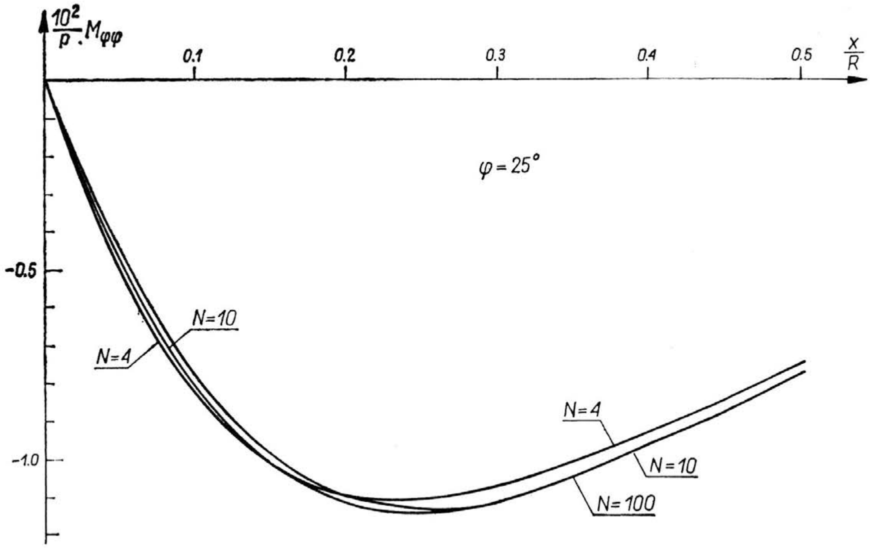

FIG. 18.

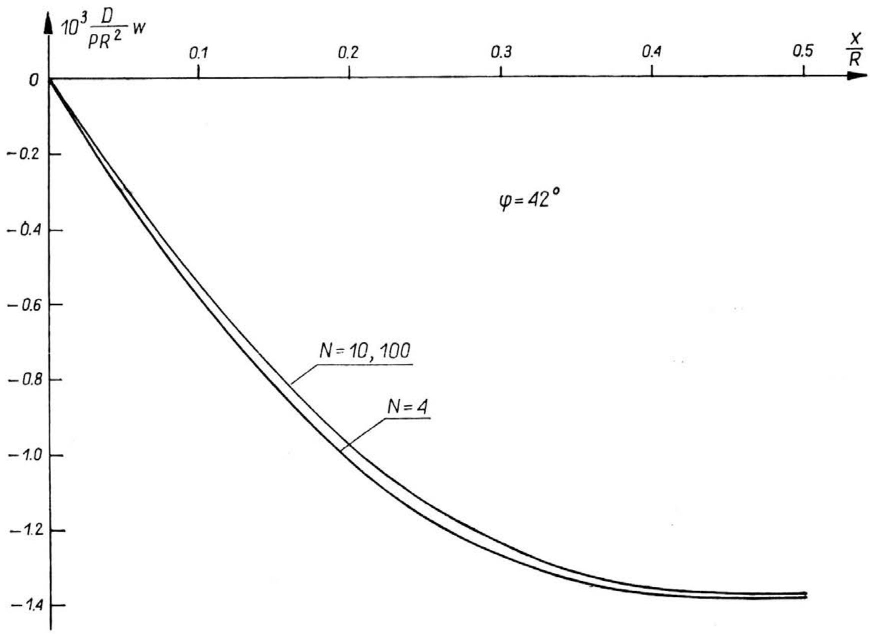

FIG. 19.

5. Conclusions

The maximum deflection w appears for $x/R \cong 0.5$ and it declines when x increases. It reaches the zero value for the first time for $x/R \cong 3$ and then oscillates about this value.

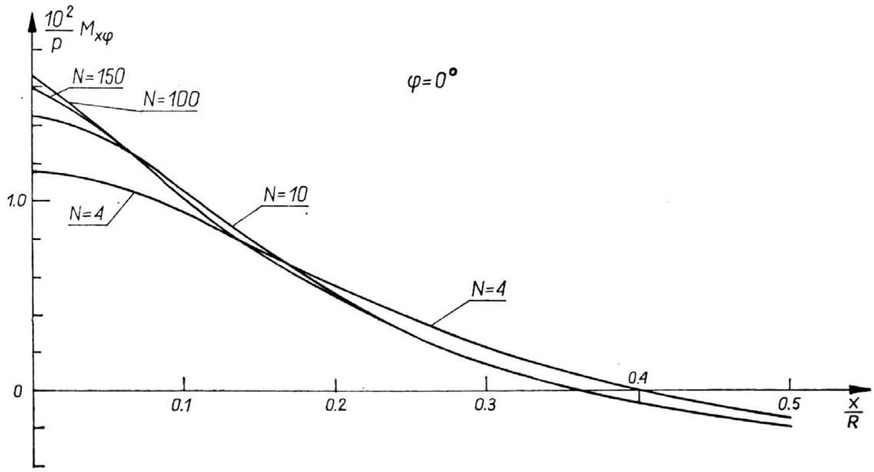

FIG. 20.

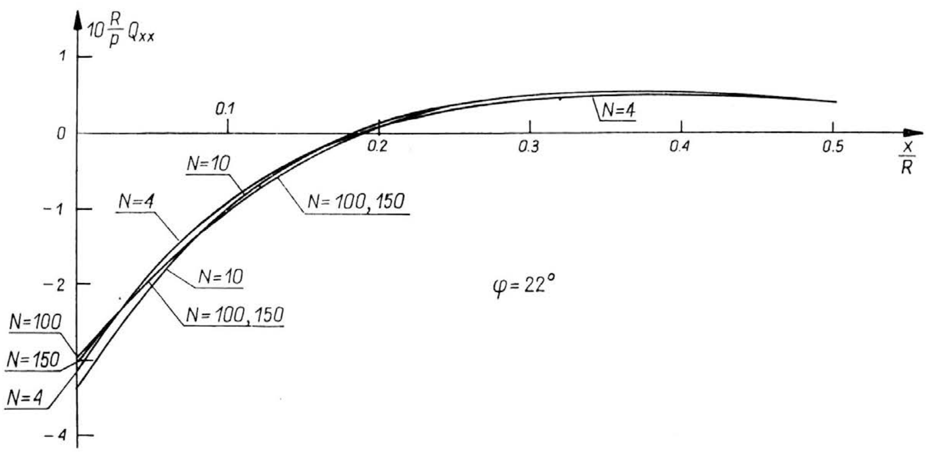

FIG. 21.

Assuming $R = 100$ [mm] and using dimensional quantities, one concludes that moment and membrane stresses are, in general, of the same order of magnitude.

It was found that if the number of forces $m = 2$, $R/h = 10$ and $x/R > 0.5$, for every component of displacements, internal moments and forces, the sufficient accuracy is obtained by taking into account only the first five nonvanishing terms of the series. When $0.1 < x/R < 0.5$, this number should vary from 5 up to 25, but even for $x/R = 0.0$ five is still the sufficient number of terms for the components v, w, M_{xx}, $M_{\varphi\varphi}$, Q_{xx}. Only in the case of $Q_{\varphi\varphi}$, $N_{\varphi\varphi}$, $N_{x\varphi}$ and for x/R less than 0.1, the summation of the series exceeded the possibilities of a quad word minicomputer used in computations.

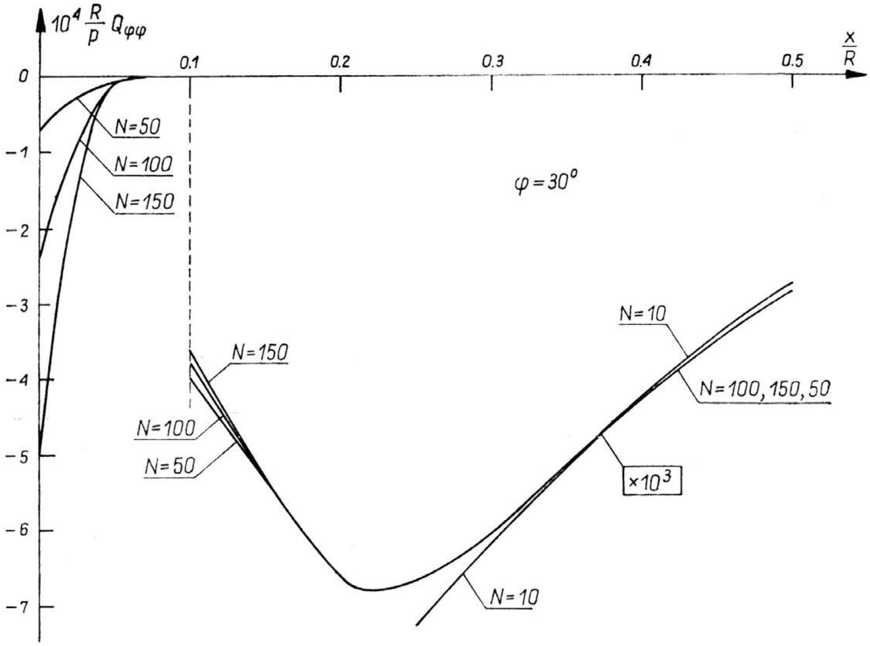

10^4 R/p Q_φφ
x/R
0
0.1
0.2
0.3
0.4
0.5
-1
-2
-3
-4
-5
-6
-7
N=50
N=100
N=150
φ=30°
N=10
N=150
N=100, 150, 50
N=100
N=50
×10^3
N=10

FIG 22.

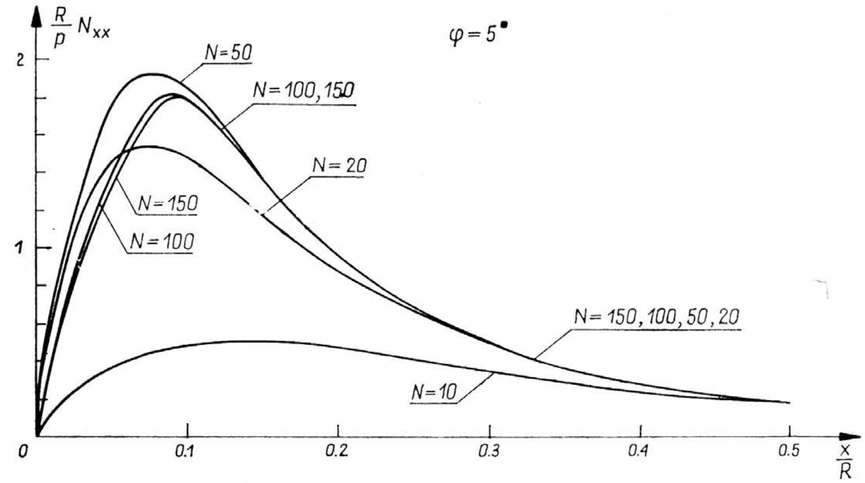

R/p N_xx
φ=5°
2
N=50
N=100, 150
N=20
N=150
1
N=100
N=150, 100, 50, 20
N=10
0
0.1
0.2
0.3
0.4
0.5
x/R

FIG. 23.

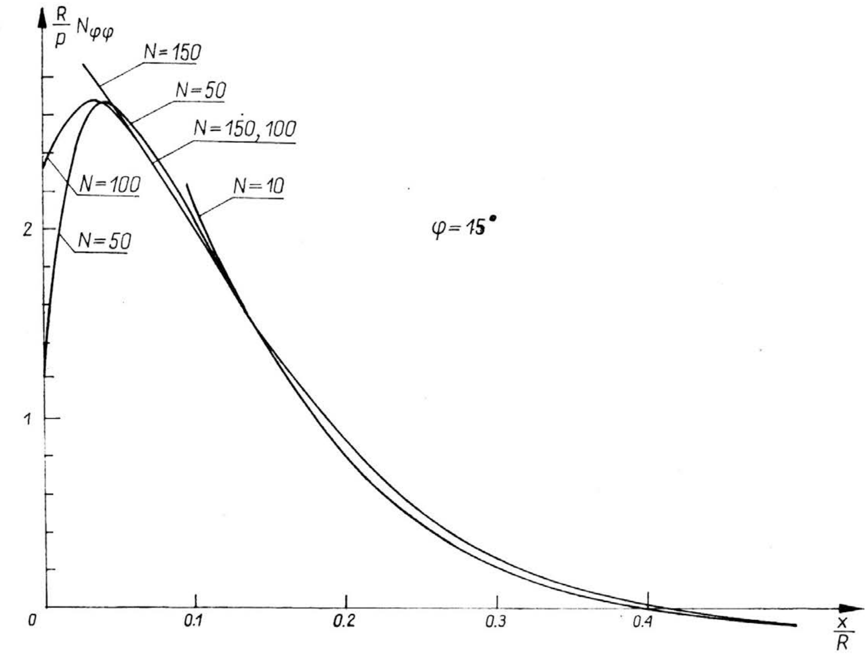

$\frac{R}{p} N_{\varphi\varphi}$
N=150
N=50
N=150, 100
N=100
N=10
N=50
$\varphi=15°$
2
1
0
0.1
0.2
0.3
0.4
$\frac{x}{R}$

FIG. 24.

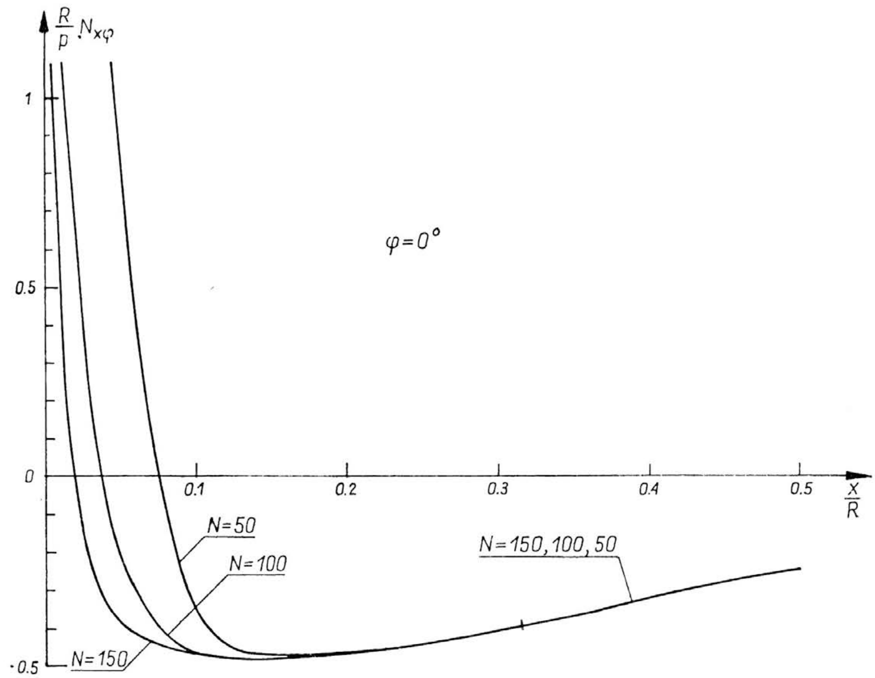

$\frac{R}{p} N_{x\varphi}$
1
$\varphi=0°$
0.5
0
0.1
0.2
0.3
0.4
0.5
$\frac{x}{R}$
N=50
N=100
N=150, 100, 50
-0.5
N=150

FIG. 25.

References

1. L. H. DONNELL, *Stability of thin-walled tubes under tortion*, NACA Report 479, 1933.
2. V. Z. VLASOV, *General theory of shells*, Moscov-Leningrad 1949 [in Russ.].
3. S. ŁUKASIEWICZ, *Complement of the equations of the technical theory of shells*, Rozpr. Inżyn., **11**, 1, 1963 [in Polish].
4. S. ŁUKASIEWICZ, *Local loads in plates and shells*, PWN, Warsaw 1979.
5. T. KACPERSKI, *Circular cylindrical shell loaded by concentrated forces normal to its free edge and tangential to middle surface*, Rozp. Inżyn., **25**, 2, 1977 [in Polish].
6. T. KACPERSKI, *Circular cylindrical shell loaded by concentrated forces normal to edge supported by means of articulated joint and tangential to middle surface*, Rozpr. Inżyn., **32**, 3, 1984 [in Polish].

DEPARTMENT OF FINE MECHANICS, WARSAW TECHNICAL UNIVERSITY
and
POLISH ACADEMY OF SCIENCES
INSTITUTE OF FUNDAMENTAL TECHNOLOGICAL RESEARCH.

Received November 29, 1984.